



**HAL**  
open science

## Two temperate corals are tolerant to low pH regardless of previous exposure to natural CO<sub>2</sub> vents

Chloe Carbonne, Núria Teixidó, Billy Moore, Alice Mirasole, Thomas Guttierrez, Jean-Pierre Gattuso, Steeve Comeau

### ► To cite this version:

Chloe Carbonne, Núria Teixidó, Billy Moore, Alice Mirasole, Thomas Guttierrez, et al.. Two temperate corals are tolerant to low pH regardless of previous exposure to natural CO<sub>2</sub> vents. *Limnology and Oceanography*, inPress, 66 (11), pp.4046-4061. 10.1002/lno.11942 . hal-03348884

**HAL Id: hal-03348884**

**<https://hal.science/hal-03348884>**

Submitted on 20 Sep 2021

**HAL** is a multi-disciplinary open access archive for the deposit and dissemination of scientific research documents, whether they are published or not. The documents may come from teaching and research institutions in France or abroad, or from public or private research centers.

L'archive ouverte pluridisciplinaire **HAL**, est destinée au dépôt et à la diffusion de documents scientifiques de niveau recherche, publiés ou non, émanant des établissements d'enseignement et de recherche français ou étrangers, des laboratoires publics ou privés.

1 **Two temperate corals are tolerant to low pH regardless of**  
2 **previous exposure to natural CO<sub>2</sub> vents**

3 Chloe Carbonne<sup>1,\*</sup>, Nuria Teixidó<sup>1,2</sup>, Billy Moore<sup>1,3</sup>, Alice Mirasole<sup>2</sup>, Thomas  
4 Gutierrez<sup>1,4</sup>, Jean-Pierre Gattuso<sup>1,5</sup>, Steeve Comeau<sup>1</sup>

5 <sup>1</sup> Sorbonne Université, CNRS, Laboratoire d'Océanographie de Villefranche, 181 chemin du Lazaret,  
6 06230 Villefranche-sur-mer, France

7 <sup>2</sup> Stazione Zoologica Anton Dohrn, Ischia Marine Centre, Department of Integrated Marine Ecology,  
8 Punta San Pietro, 80077, Ischia (Naples), Italy

9 <sup>3</sup> MSc Tropical Marine Biology, University of Essex, Wivenhoe Park, Colchester CO4 3SQ, United  
10 Kingdom

11 <sup>4</sup> Master Science de la Mer, Aix-Marseille Université, 58 bd Charles Livon, 13284 Marseille Cedex  
12 07, France

13 <sup>5</sup> Institute for Sustainable Development and International Relations, Sciences Po, 27 rue Saint  
14 Guillaume, F-75007 Paris, France

15 \*Corresponding author: [chloe.carbonne@imev-mer.fr](mailto:chloe.carbonne@imev-mer.fr)

16 Running head: Coral tolerance to ocean acidification

17 Keywords: ocean acidification, CO<sub>2</sub> vents, temperate, Mediterranean, coral, *Cladocora*  
18 *caespitosa*, *Astroides calycularis*, calcification, tolerance, low pH

19

20

21

22

23

24 **Abstract**

25 Ocean acidification is perceived to be a major threat for many calcifying organisms, including  
26 scleractinian corals. Here we investigate (1) whether past exposure to low pH environments  
27 associated with CO<sub>2</sub> vents could increase corals tolerance to low pH and (2) whether  
28 zooxanthellate corals are more tolerant to low pH than azooxanthellate corals. To test these  
29 hypotheses, two Mediterranean colonial corals *Cladocora caespitosa* (zooxanthellate) and  
30 *Astroides calycularis* (azooxanthellate) were collected from CO<sub>2</sub> vents and reference sites and  
31 incubated in the laboratory under present-day (pH on the total scale, pH<sub>T</sub> 8.07) and low pH  
32 conditions (pH<sub>T</sub> 7.70). Rates of net calcification, dark respiration and photosynthesis were  
33 monitored during a six-month experiment. Monthly net calcification was assessed every 27 to  
34 35 d using the buoyant weight technique, whereas light and dark net calcification was  
35 estimated using the alkalinity anomaly technique during 1 h incubations. Neither species  
36 showed any change in net calcification rates, respiration, and photosynthesis regardless of  
37 their environmental history, pH treatment and trophic strategy. Our results indicate that *C.*  
38 *caespitosa* and *A. calycularis* could tolerate future ocean acidification conditions for at least 6  
39 months. These results will aid in predicting species' future responses to ocean acidification,  
40 and thus improve the management and conservation of Mediterranean corals.

41

42

43

44

45

46

47

## 48 **Introduction**

49 Ocean acidification describes the shift in carbonate chemistry caused by the uptake of  
50 anthropogenic CO<sub>2</sub> by the ocean (Caldeira and Wickett 2003, Gruber et al. 2019). It causes an  
51 increase in dissolved inorganic carbon and bicarbonate ion concentrations, along with a  
52 concurrent decrease in pH, carbonate ion concentration and its associated saturation state ( $\Omega$ ;  
53 Orr et al. 2005). Calcifying species are perceived to be particularly vulnerable to ocean  
54 acidification (Kroeker et al. 2013a). For example, corals are particularly sensitive to changes  
55 in carbonate chemistry as their skeleton is made of aragonite, a metastable form of calcium  
56 carbonate that is less stable than calcite (Erez et al. 2011, Foster and Clode 2016). As a result,  
57 coral calcification is expected to decrease as seawater acidity increases (Gattuso et al. 1999).  
58 Coral calcification decreases by on average 22% under pH values expected by the end of the  
59 century under the high-CO<sub>2</sub> emissions scenario (RCP 8.5 from AR5 of IPCC; Chan and  
60 Connolly 2013). However, a range of contradictory species- and experience-specific  
61 responses have been described (e.g. Kornder et al. 2018), with some species such as massive  
62 *Porites* spp. being tolerant to ocean acidification (Fabricius et al. 2011). This resistance to  
63 ocean acidification was also described in several temperate and cold-water corals (e.g.  
64 Rodolfo-Metalpa et al. 2010). Such tolerance is seen in many studied parameters such as net  
65 calcification rate, respiration, photosynthetic physiology, calcifying fluid pH (McCulloch et  
66 al. 2012a, Wang et al. 2020). According to Varnerin et al. (2020) even juveniles from the  
67 temperate *Oculina arbuscula* were only slightly affected by ocean acidification.

68 A central question when assessing the future of corals in a high-CO<sub>2</sub> world is whether they  
69 have the capacity to acclimatize and further adapt to ocean acidification. This question  
70 remains unanswered as corals are generally long-lived organisms for which it is extremely  
71 challenging to study acclimatization and adaptation processes over several generations.

72 Acclimatization refers to reversible phenotypic changes limited by genotype, occurring under

73 naturally varying conditions by a physiological readjustment of the organism's tolerance  
74 levels (Edmunds and Gates 2008). In contrast, adaptation refers to changes in the genetic  
75 composition of a population by natural selection, in which traits will be passed on to the next  
76 generation (Savolainen et al. 2013). In a recent study, Cornwall et al. (2020) conducted a one-  
77 year experiment showing that coralline algae have the capacity to acclimatize to low pH after  
78 seven generations of exposure. Replicating such a study on corals is virtually impossible as  
79 they are long-lived organisms which only reach sexual maturity after several years. CO<sub>2</sub> vents  
80 therefore offer a unique opportunity to investigate the response of corals to ocean acidification  
81 over long periods of time. In such systems, volcanic CO<sub>2</sub> bubbles from the seafloor which  
82 acidifies the surrounding seawater and creates an environment, with carbonate chemistry  
83 conditions that mimic those expected in the future (Hall-Spencer et al., 2008, Camp et al.  
84 2018, González-Delgado and Hernández 2018). By investigating individuals, species, and  
85 communities along transects radiating from the sources of CO<sub>2</sub>, it is possible to substitute time  
86 for space. It must be pointed out, however, that CO<sub>2</sub> vents are imperfect windows into the  
87 future because they generally do not mimic other climate-related changes such as ocean  
88 warming. Furthermore, it is not possible to disentangle any changes in the mean versus  
89 variability of seawater pH (Hall-Spencer et al. 2008). Overall, these systems exhibit  
90 significant decreases in trophic complexity and biodiversity, as well as a major decrease in the  
91 abundance of calcifying organisms (Kroeker et al. 2013b, Linares et al. 2015, Teixidó et al.  
92 2018). Corals living in the vicinity of CO<sub>2</sub> vents have been exposed to low and high  
93 variability pH conditions for an extended period of time (years to decades). They are therefore  
94 ideal models to investigate acclimatization and adaptation to ocean acidification (Fantazzini et  
95 al. 2015, Foo et al. 2018). Populations or individuals living in these variable and more  
96 extreme environments are hypothesized to be more tolerant to suboptimal environmental  
97 conditions such as acidification (e.g. Cornwall et al. 2018).

98 CO<sub>2</sub> vents have been used for transplant experiments between acidified and nearby reference  
99 sites with ambient pH and no vent activity. For example, a decline in calcification was  
100 described in the zooxanthellate corals *Cladocora caespitosa* and *Balanophyllia europaea*  
101 transplanted to a CO<sub>2</sub> vent site in Ischia (Rodolfo-Metalpa et al. 2011). The skeletal growth of  
102 *Porites astreoides* living in a natural pH gradient showed no acclimatization to ocean  
103 acidification despite their life-long exposure to low pH (Crook et al. 2013). Few laboratory  
104 studies have focused on temperate scleractinian corals from natural CO<sub>2</sub> vents despite the  
105 relevance of studying the tolerance of temperate coral populations to ocean acidification  
106 (Trotter et al. 2011, Teixidó et al. 2020). Such studies are important for understanding and  
107 elucidating how these species will respond to the suboptimal pH conditions projected for the  
108 end of this century.

109 The symbiosis between scleractinian corals and endosymbiotic algae, commonly referred to  
110 as zooxanthellae, has been studied thoroughly (Davy et al. 2012). Photosynthetic products  
111 from zooxanthellae contribute significantly to the energy budget of the scleractinian host  
112 (Allemand et al. 2011, Muller-Parker et al. 2015) and can play an important role in  
113 calcification (Erez et al. 2011, Inoue et al. 2018). However, not all corals harbor  
114 zooxanthellae (azooxanthellate corals). Gibbin et al. (2014) demonstrated that zooxanthellae  
115 regulate intracellular pH under acidified conditions, whereas azooxanthellate corals can suffer  
116 from reduced intracellular pH which can lead to intracellular acidosis. It can thus be expected  
117 that photosynthesis may enhance calcification by (1) providing energy for this energetically  
118 costly process and (2) by increasing pH at the site of calcification (Allemand et al. 2011). In a  
119 transplant experiment in the CO<sub>2</sub> vents of Panarea, Prada et al. (2017) showed that the  
120 calcification of two azooxanthellate corals *Leptopsammia pruvoti* and *Astroides calycularis*  
121 decreased at low pH, whereas calcification of the zooxanthellate coral *B. europaea* was  
122 unaffected. A similar result was observed in pH-controlled aquaria by Ohki et al. (2013) as

123 polyps of *Acropora digitifera* with symbionts showed higher calcification rates than polyps  
124 without symbionts under low pH, suggesting that symbionts confer tolerance to ocean  
125 acidification. However, in a study led by McCulloch et al. (2012b), azooxanthellate cold-  
126 water corals presented higher intracellular pH regulation than shallow-water zooxanthellate  
127 corals under acidification. As it is not truly known whether or not symbionts promote the  
128 maintenance of elevated pH at the site of calcification, it is interesting to compare  
129 zooxanthellate and azooxanthellate corals as they may display contrasting responses to ocean  
130 acidification.

131 The present study focuses on two Mediterranean long-lived corals of key relevance for  
132 conservation, the zooxanthellate species *C. caespitosa* (Linnaeus, 1767) and the  
133 azooxanthellate species *A. calycularis* (Pallas, 1766). *Cladocora caespitosa* is a unique  
134 zooxanthellate reef-building coral that provides a valuable ecosystem service in the  
135 Mediterranean Sea which is lacking large bioconstructions (Kersting and Linares 2012).  
136 *Astroides calycularis* is commonly found in the southwestern Mediterranean Sea and can be  
137 highly abundant in low light, shallow rocky habitats (Zibrowius 1995). These two  
138 scleractinian corals naturally occur at two newly discovered CO<sub>2</sub> vent systems along the coast  
139 of Ischia, Italy. In situ data obtained by Teixidó et al. (2020) showed variable responses in  
140 skeletal structure and growth patterns of *A. calycularis*, with colonies from the CO<sub>2</sub> vent site  
141 characterized by smaller size, fewer polyps, and less porous, denser skeletons. Thus, these  
142 two scleractinian coral species grown under elevated pCO<sub>2</sub> environments are great model  
143 systems for assessing tolerance to acidification. Here, two hypotheses are tested: (1) past  
144 exposure to low pH conditions confers tolerance to ocean acidification and (2) the coral-algal  
145 symbiosis modulates this tolerance. To test these hypotheses, corals from natural CO<sub>2</sub> vent  
146 systems and reference sites were exposed to present-day (pH on the total scale, pH<sub>T</sub> ~ 8.07)

147 and low pH conditions ( $\text{pH}_T \sim 7.70$ ) during a six-month long laboratory experiment, in which  
148 calcification, respiration and photosynthesis rates were assessed.

## 149 **Material and Methods**

### 150 Study sites

151 We studied populations of the corals *Cladocora caespitosa* and *Astroides calycularis* that  
152 naturally occur at two distinct  $\text{CO}_2$  vent sites with low pH, and two reference sites with  
153 ambient pH and no vent activity at the island of Ischia, Italy (Fig. S1 Supplementary  
154 materials). *Cladocora caespitosa* occurs near a  $\text{CO}_2$  vent site adjacent to rocky reefs at about  
155 10 m depth (Chiane del Lume, hereafter Vent 1), whereas *A. calycularis* occurs in another  
156  $\text{CO}_2$  vent site between 1 - 2 m depth (Grotta del Mago, a semi-submerged cave hereafter Vent  
157 2, where  $\text{CO}_2$  vents occur at 5 m depth). Vent gas compositions at Vent 1 and Vent 2 were  
158 predominantly  $\text{CO}_2$  (mean  $\pm$  SE:  $93.9 \pm 0.6$  for Vent 1,  $93.4 \pm 1.0$  for Vent 2), with  
159 undetectable levels of hydrogen sulfide ( $< 0.0002\%$ ), and did not elevate the temperature (for  
160 more information on gas measurements, see Teixidó et al. 2020). The reference sites without  
161 any visible vent activity and exhibiting ambient pH were located: i) approximately 100 m  
162 west from Vent 1 for *C.caespitosa* (hereafter Ambient 1, 10 m depth) and ii) 1.5 km away  
163 from Vent 2 for *A. calycularis* (San Pancrazio, an overhang, hereafter Ambient 2, 1-2 m  
164 depth) (Fig. S1 Supplementary materials).

### 165 Coral field surveys

166 The *C. caespitosa* abundance was quantified using 12 quadrats of 50 cm x 50 cm, which were  
167 randomly placed along the rocky reef at 10 m depth at the two sites ( $n = 24$  quadrats in total).  
168 Abundance was assessed by counting the number of colonies found in each quadrat. In  
169 addition, size of colonies was determined by measuring the major colony diameter with a

170 plastic ruler (with an error of  $\pm 1$  cm) (Peirano et al. 2001). Major colony diameter was  
171 selected as the best colony size descriptor (Kersting 2012). The *A. calycularis* abundance was  
172 quantified using 12 photo-quadrats (25 x 25 cm) between 1 and 2 m depth in the two other  
173 sites ( $n = 24$  quadrats in total, Vent 2, Ambient 2). Size frequency-distribution was calculated  
174 by counting the number of polyps of each colony and each colony was then pooled into one of  
175 five size classes (I: 1-5 polyps; II: 6-10 polyps; III: 11-15 polyps; IV: 16-20 polyps; V:  $> 20$   
176 polyps). The survey's depth for *C. caespitosa* and *A. calycularis* corresponded to the depth  
177 range at which colonies were sampled for the experiment (see below). Abundance and size-  
178 frequency data for *A. calycularis* have been described previously in Teixidó et al. (2020).

#### 179 In situ pH<sub>T</sub> and carbonate chemistry associated with CO<sub>2</sub> vents and ambient pH sites

180 SeaFET<sup>TM</sup> Ocean pH sensors (Satlantic) were deployed to quantify variation in pH at the two  
181 CO<sub>2</sub> vent and the two ambient pH sites. Measurements were taken every 15 minutes. One sensor  
182 was deployed at the Vent 1 site from May 7 to 21, 2019, and one sensor was deployed at the  
183 Ambient 1 site during the same period. At the semi-submerged cave (Vent 2), sensors were  
184 deployed in May-June 2019 (before summer) and in September 2018 (after summer). Dates of  
185 deployment for Vent 2 were from September 8 to September 24, 2018 and from May 30 to June  
186 18, 2019 at Vent 2. One sensor was deployed in the reference area Ambient 2 during the same  
187 period. Before deployment, the SeaFETs were calibrated with ambient pH water in the  
188 aquarium facilities at the Center Villa Dohrn (Ischia, Italy). The mean offset between  
189 calibration samples and calibrated SeaFET pH was  $\pm 0.002$  units, indicating high quality pH  
190 dataset. Discrete water samples were collected using Niskin bottles to measure the carbonate  
191 system parameters during the pH sensor deployment. Samples for total alkalinity ( $A_T$ ) were  
192 collected using standard operating protocols. The HCl (0.1 M) titrant solution was calibrated  
193 against certified reference materials distributed by A.G. Dickson (CRM, Batches #153, #171,  
194 and #177). Precision of the  $A_T$  measurements of CRMs was  $< 2$  and  $< 1 \mu\text{mol kg}^{-1}$  from nominal

195 values.  $A_T$  and  $pH_T$  were used to determine the remaining carbonate system parameters at in  
196 situ temperature and depth of each sampling period in the R package seacarb v3.2.12. For full  
197 details of pH sensors deployment, calibration, and total alkalinity standard operating protocols,  
198 see Teixidó et al. (2020).

#### 199 Coral collection

200 A total of 81 colonies of *C. caespitosa* and *A. calycularis* were randomly sampled for the  
201 aquarium experiment. Fourteen (Vent 1) and sixteen (Ambient 1) colonies of *C. caespitosa*  
202 were collected at 10 m depth; twenty-seven (Vent 2) and fourteen (Ambient 2) colonies of *A.*  
203 *calycularis* were collected from 1 to 2 m depth. A portion of approximately 3 x 3 cm was  
204 gently dislodged from each colony using a hammer and chisel. They were placed in coolers  
205 filled with seawater changed regularly and maintained in Ischia for two days prior to  
206 transportation to the aquarium facilities of the *Laboratoire d'Océanographie de Villefranche*,  
207 France. The duration of the transfer was less than 10 h; colonies were wrapped in seawater-  
208 soaked paper tissues. The colonies were cleaned, tagged with a number stuck under it using  
209 water-resistant epoxy glue, and maintained at an ambient  $pH_T$  of ~8.05 during 2 weeks.

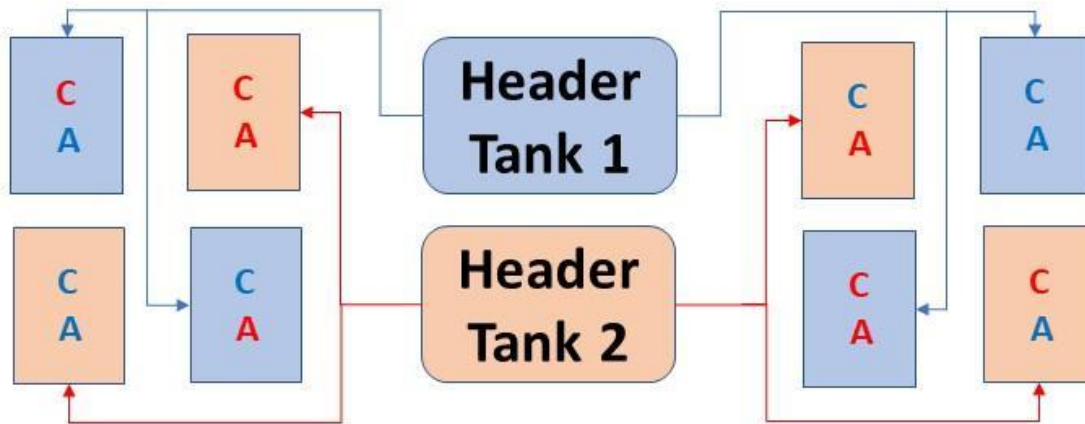
#### 210 Experimental set-up and treatments

211 Colonies of *C. caespitosa* and *A. calycularis* were maintained in two constant pH treatments  
212 during six months (202 days), one “present-day” treatment with a  $pH_T = 8.08 \pm 0.01$  (mean  $\pm$   
213 SE,  $n = 348$ , total number of weekly  $pH_T$  measures in each 12 present-day experimental tank)  
214 and one “low pH” treatment with a  $pH_T = 7.72 \pm 0.01$  (mean  $\pm$  SE,  $n = 348$ , total number of  
215 weekly  $pH_T$  measures in each 12 low pH experimental tank) corresponding to the pH values  
216 expected by the end of the century under the RCP 8.5 CO<sub>2</sub> emissions scenario. More  
217 specifically, 14 colonies from Vent 1 and 16 colonies from Ambient 1 of *C. caespitosa* and 27  
218 from Vent 2 and 14 from Ambient 2 of *A. calycularis* were used for this experiment. The vent-

219 low pH condition was used to test the acclimation or long-term tolerance of the colonies to  
220 low pH in the lab, after a life-time of exposure to in situ low pH. The ambient-low pH  
221 condition was used to test the short-term tolerance to low pH of colonies that have not been  
222 exposed to low pH before. The vent-present day condition tested the response to ambient pH  
223 of colonies exposed in the long-term to in situ low pH. The ambient-present day condition  
224 was the control. There were six independent 5 L experimental tanks for each of the four  
225 conditions (origin x pH treatment), for a total of 24 experimental tanks. Each experimental  
226 tank contained one to three colonies of each species, depending on their size, to get  
227 approximately the same total amount of polyps per tank (Tab. S1 Supplementary materials).  
228 Seawater pumped from Villefranche Bay at 5 m depth was continuously flowing into six 25 L  
229 header tanks, used as water storage and to maintain gravity pressure for water flow into the  
230 experimental tanks. Three header tanks were maintained at  $\text{pH}_T \sim 8.07$  (present-day  
231 treatment) and the other three at  $\text{pH}_T \sim 7.7$  (low pH treatment). pH was controlled in the  
232 header tanks using pH controllers (APEX, Neptune Systems) which regulated the delivery of  
233 pure  $\text{CO}_2$ . Each header tank gravity-fed four experimental four-liter tanks at a rate of  $100 \text{ ml}$   
234  $\text{min}^{-1}$  (Fig. 1).

235 Light was provided by 89 W LED light bars (Aquaristik, Aqualumix). Irradiance gradually  
236 increased from 0 at 06:00 to a maximum irradiance of  $180 \mu\text{mol photons m}^{-2} \text{ s}^{-1}$  between  
237 11:00 and 14:00, and gradually decreased to 0 at 18:00. According to the attenuation  
238 coefficients of PAR in Villefranche Bay calculated in Martin and Gattuso (2009), the  
239 maximum irradiance levels used in the study ( $180 \mu\text{mol photons m}^{-2} \text{ s}^{-1}$ ) is within the  
240 irradiance range observed at 10 m, where *Cladocora caespitosa* can be found in the  
241 Mediterranean Sea ( $154$  to  $449 \mu\text{mol photons m}^{-2} \text{ s}^{-1}$ ). As *A. calycularis* were collected in a  
242 semi-submerged cave and an overhang, dark plastic bags covered one side of the experimental  
243 tanks to shade colonies from direct light. The 24 experimental tanks were kept in 6 water

244 baths under controlled temperature following Ischia's natural changes (Fig. S2 Supplementary  
 245 materials, APEX, Neptune Systems). Submersible pumps (NEWA) provided water motion in  
 246 each experimental tank. Three times a week, each tank was provided with a 30 mL solution of  
 247 freshly hatched brine shrimps (*Artemia* sp.) for feeding.



**x 3 replicates**

<u>pH treatment</u>	<u>Origin</u>	<u>Species</u>
<span style="display: inline-block; width: 15px; height: 15px; background-color: #add8e6; border: 1px solid black;"></span> Present day	Ambient	C <i>Cladocora caespitosa</i>
<span style="display: inline-block; width: 15px; height: 15px; background-color: #ffcc99; border: 1px solid black;"></span> Low pH	Vent	A <i>Astroides calycularis</i>

248 **Figure 1. Experimental set-up used to test the effects of origin (ambient vs vent site) and**  
 249 **pH treatment (present day,  $pH_T = 8.07 \pm 0.01$  and low pH,  $pH_T = 7.72 \pm 0.01$ ) on the**  
 250 **coral *C. caespitosa* and *A. calycularis*.** The experimental set-up was repeated 3 times,  
 251 resulting in 6 header tanks, and 24 experimental tanks in which corals were randomly  
 252 assigned.

253 Health status of experimental colonies

254 With pictures at the start of the experiment, each colony has been classified into two  
 255 categories: colonies with loss of coenosarc (tissue between polyps) and colonies with tissue  
 256 connecting their polyps. The number of dead polyps per colony (complete disappearance of  
 257 tissue in the calice) was counted by comparing the pictures of the same colony at the start and  
 258 the end of the experiment.

## 259 Carbonate chemistry in experimental tanks

260 pH in the header and experimental tanks was measured weekly using a handheld pH-meter  
261 (826 pH mobile, Metrohm) calibrated with a TRIS buffer (batch #T33 provided by A.  
262 Dickson, Scripps Institution of Oceanography, USA) before each set of measurements. Total  
263 alkalinity ( $A_T$ ) of each experimental and header tank was measured weekly during the first  
264 four weeks in order to ascertain whether conditions were altered by metabolic activity.  
265 Subsequently, and for the remainder of the experiment,  $A_T$  was measured every month in four  
266 randomly selected tanks and one header.  $A_T$  was determined by potentiometric titration using  
267 a Metrohm 888 Titrando following the method of (Dickson et al. 2007). Titrations of certified  
268 reference material (Batch #186) provided by A. Dickson were used to assess the accuracy of  
269 the measurements and were within  $6.5 \mu\text{mol kg}^{-1}$  of the reference value. Ischia's temperatures  
270 are between  $0.87$  to  $2.67^\circ\text{C}$  higher than in the Bay of Villefranche during the studied period.  
271 Water pumped on the Bay of Villefranche was heated to be as close as possible to Ischia's  
272 temperatures. Salinity at Ischia and in the Bay of Villefranche-sur-Mer are similar. Salinity  
273 data were gathered from the salinity recorded weekly in the Bay of Villefranche by the  
274 *Service d'Observation Rade de Villefranche, SO-Rade*, of the *Observatoire Océanologique*  
275 *and the Service d'Observation en Milieu Littoral, SOMLIT/CNRS-INSU*.  $\text{pH}_T$ , temperature,  $A_T$   
276 and salinity were used to calculate the other carbonate chemistry parameters using the R  
277 package seacarb (Gattuso et al. 2020) (Tab. 1, Tab. S2 Supplementary materials).

## 278 Six-month and monthly calcification

279 Calcification rate was assessed using the buoyant weight technique (Davies 1989). Weighing  
280 was done every 27 to 35 days. Changes in wet weight were converted to dry weight using the  
281 following equation:

282 
$$dry\ weight = \frac{wet\ weight}{(1 - \frac{water\ density}{aragonite\ density})}$$

283 with an aragonite density of 2.93 g cm<sup>3</sup>. Six-month calcification rates corresponding to the  
284 entire experiment duration were determined as the change in dry weight between the first and  
285 the last weighing, normalized by the corals living tissue surface at the end of the experiment  
286 and the number of days of the experiment (202 days). Regular rates of calcification over time  
287 were normalized to the surface of the corals and to the number of days between weighing  
288 (~30 d). Surfaces were determined by the aluminum foil technique for *C. caespitosa* (Marsh  
289 1970) because these 3D colonies were impossible to analyze with 2D pictures. *A. calycularis*  
290 surfaces were measured by photographic analysis with the software ImageJ for (IMAGEJ,  
291 NIH US Department of Health and Human Services) as they had flat shape. Surface  
292 measurements were completed at the start and end of the experiment. Marginal changes in  
293 surface area were observed between the beginning and end of the experiment.

294 Dark respiration, gross photosynthesis and short-term calcification

295 Dark respiration, net photosynthesis and short-term calcification were determined during less  
296 than 1 h incubations in 500 ml transparent perspex chambers, placed in a temperature-  
297 controlled water bath to maintain a constant temperature. Incubations were carried out a  
298 month after the start of the experiment (hereafter “start”) and a month before the end of the  
299 experiment (hereafter “end”) at the same temperature of 20°C. Magnetic stirrers were used to  
300 provide water motion in the incubation chambers. Each colony was transferred to an  
301 individual chamber filled with water from the experimental tanks from which the corals were  
302 taken for the incubation. A blank incubation with no coral colony and filled with water from  
303 the same header tank was performed for each four experimental tanks. Incubations lasted 30  
304 to 60 min depending on the magnitude of the metabolic activity. To measure oxygen uptake

305 during respiration, colonies were maintained in darkness by covering the chamber with an  
306 opaque plastic bag and incubations started after a 10 min acclimation period. Production of  
307 oxygen by photosynthesis was only measured on colonies of *C. caespitosa* under an  
308 irradiance of  $180 \mu\text{mol photons m}^2 \text{s}^{-1}$ . Oxygen saturation within the chambers was measured  
309 every 5 s using a fiber optic oxygen sensor (PreSens, OXY-4 mini), which was calibrated at  
310 0% saturation in an oxygen-free solution created by saturating seawater with sodium sulfite,  
311 and at 100% saturation in an oxygen-saturated seawater obtained by bubbling ambient air  
312 during 5 min. The difference in oxygen saturation between the beginning and end of the  
313 incubation was converted to  $\text{O}_2 \text{ mg L}^{-1}$  using the `gas_O2sat` function of the `marelac R` package  
314 (Soetaert et al. 2020). Oxygen consumption was then normalized by coral surface area,  
315 incubation time and chamber volume to obtain the rates of respiration (negative in dark  
316 conditions) and net photosynthesis (oxygen production in excess of the respiratory demand  
317 under light conditions). The rate of gross photosynthesis was calculated by subtracting the  
318 respiration rate in dark to the rate of net photosynthesis, with the assumption that respiration  
319 rate is the same under light and dark conditions.

320 Water samples were collected at the beginning and end of the incubation for each colony for  
321 calcification determination using the alkalinity anomaly technique (Smith and Key 1975).  
322 This method relies on the stoichiometric relationship between total alkalinity and  
323 calcification, where the precipitation of one mole of  $\text{CaCO}_3$  lowers the total alkalinity by two  
324 moles. Alkalinity anomalies were normalized by the coral surface area, incubation time, and  
325 chamber volume to calculate light and dark calcification rates. The alkalinity anomaly method  
326 was only applied to the zooxanthellate *C. caespitosa*.

327

328

## 329 Data analysis

330 *Biological surveys:* A generalized linear mixed model was used to test for differences in  
331 abundance (poisson family) as a function of site (fixed factor, 2 levels) and quadrat as a  
332 random effect. Chi-square contingency tables were used to compare the size–frequency  
333 distributions between sites. *Laboratory experiment:* The assumptions of normality and  
334 equality of variance were evaluated through graphical analyses of residuals using QQ plot  
335 functions in R software. Mean values of the colonies in the experimental tank were used as a  
336 replicate for six-month calcification. Each incubation was treated as a statistical replica  
337 because they were done in individual chambers on single individuals. The effect of header  
338 tanks was first tested with an ANOVA and since its significance was negligible ( $p > 0.05$ ), it  
339 was not considered in subsequent analyses. A two way-ANOVA was then used to test for  
340 differences in net calcification caused by the origin (vent or ambient pH sites) and the pH  
341 treatments (present-day or low pH) for both *C. caespitosa* and *A. calyularis*. For net  
342 calcification as a function of time, a three-way ANOVA was applied, with origin, pH  
343 treatment, and time as fixed factors. Tukey’s post hoc tests were conducted when significant  
344 differences were detected. Three-way repeated measure ANOVA was used for dark  
345 respiration, gross photosynthesis and short-term calcification since the same colonies of *C.*  
346 *caespitosa* and *A. calyularis* were used at the start and end of the incubations. Results have  
347 been reported as means  $\pm$  standard error of the mean (SE) hereafter, unless otherwise noted.

## 348 **Results**

### 349 In situ environmental conditions and populations of corals

350 Water carbonate chemistry and in situ monitoring of seawater pH<sub>T</sub> (pH on the total scale) at  
351 the CO<sub>2</sub> vent and reference sites with ambient pH showed mean pH<sub>T</sub> = 7.91 at Vent 1, pH<sub>T</sub> =  
352 7.91 at Vent 2, pH<sub>T</sub> = 8.05 at Ambient 1, and pH<sub>T</sub> = 7.97 at Ambient 2, respectively (Tab. 1).

353 The field surveys showed significant lower abundance of *C. caespitosa* at Vent 1 compared to  
354 Ambient 1 ( $1.8 \pm 0.16$  colonies versus  $3.3 \pm 0.35$ ,  $Z = 2.2$ ,  $p < 0.02$ , Fig. S3 Supplementary  
355 materials). No large colonies of more than 21 cm were found at Vent 1 (Fig. S1,  
356 Supplementary materials). This reduction of size was also observed for *A. calycularis* at Vent  
357 2 (92 % had up to 10 polyps versus 72 % in Ambient 2), which differed significantly between  
358 sites ( $\chi^2 = 76.7$ ,  $p < 0.0001$ ). Abundance of *A. calycularis* was lower in Vent 2 ( $67.1 \pm 10.3$  at  
359 Vent 2 versus  $80.3 \pm 14.5$  at Ambient 2,  $Z = 2.65$ ,  $p < 0.08$ ).

360

361 **TABLE 1. Measured and estimated seawater physiochemical parameters at the CO<sub>2</sub> vent sites, reference areas with ambient pH and both pH treatment**  
362 **in the experimental tanks for salinity (S), temperature (T), total alkalinity (AT), dissolved inorganic carbon (C<sub>T</sub>), pH<sub>T</sub>, pCO<sub>2</sub>, calcite (Ω<sub>c</sub>) and aragonite**  
363 **(Ω<sub>a</sub>) saturation.** Values are means ± SD with 25<sup>th</sup> and 75<sup>th</sup> percentiles. Calculated concentrations of C<sub>T</sub>, pCO<sub>2</sub>, Ω<sub>c</sub> and Ω<sub>a</sub> are shown. 1: Parameters measured  
364 from discrete water samples; 2: parameters measured with in situ sensors. pH conditions: vent system (low pH); ambient pH; ambient pH experimental treatment  
365 (present day); acidified pH experimental treatment (low pH).

Local name	pH conditions	S	T (°C)	A <sub>T</sub> (μmol kg <sup>-1</sup> )	C <sub>T</sub> (μmol kg <sup>-1</sup> )	pH <sub>T</sub>	pCO <sub>2</sub> (μatm)	Ω <sub>c</sub>	Ω <sub>a</sub>
Vent1	Low pH	37.9 <sup>1</sup> ± 0	16.8 <sup>2</sup> ± 0.4	2532 <sup>1</sup> ± 16	2324 ± 47	7.91 <sup>2</sup>	626 ± 311	3.69 ± 0.61	2.39 ± 0.39
		(37.9, 37.9), n=3	(16.6, 17.1), n=1326	(2522, 2545), n=25	(2292, 2341), n=1326	(7.89, 7.99), n=1326	(497, 643), n=1326	(3.43, 4.13), n=1326	(2.22, 2.67), n=1326
Ambient 1	Ambient pH	37.3 <sup>1</sup> ± 0	17.3 <sup>2</sup> ± 0.4	2618 <sup>1</sup> ± 15	2338 ± 20	8.05 <sup>2</sup>	448 ± 42	4.80 ± 0.30	3.11 ± 0.19
		(37.2, 37.3), n=3	(17.0, 17.6), n=1331	(2607, 2633), n=14	(2324, 2350), n=1331	(8.03, 8.07), n=1331	(417, 471), n=1331	(4.61, 5.01), n=1331	(2.98, 3.24), n=1331
Vent 2 (Sept 2018)	Low pH	37.3 <sup>1</sup> ± 0.2	25.9 <sup>2</sup> ± 0.2	2564 <sup>1</sup> ± 7	2542 ± 79	7.65 <sup>2</sup>	2905 ± 1664	1.68 ± 0.59	1.11 ± 0.39
		(37.2, 37.5), n=9	(25.8, 26.0), n=1530	(2561, 2566), n=9	(2477, 2585), n=1530	(7.58, 7.90), n=1530	(1724, 3438), n=1530	(1.21, 2.21), n=1530	(0.80, 1.47), n=1530
Vent 2 (June 2019)	Low pH	37.8 <sup>1</sup> ± 0	21.8 <sup>2</sup> ± 2.1	2541 <sup>1</sup> ± 20	2352 ± 89	7.74 <sup>2</sup>	983 ± 868	3.56 ± 1.05	2.33 ± 0.69
		(37.8, 37.8), n=7	(19.8, 23.8), n=1841	(2533, 2550), n=7	(2289, 2389), n=1841	(7.74, 7.93), n=1841	(590, 978), n=1841	(2.96, 4.39), n=1841	(1.94, 2.88), n=1841
Ambient 2	Ambient pH	37.9 <sup>1</sup> ± 0	26.4 <sup>2</sup> ± 1	2642 <sup>1</sup> ± 17	2324 ± 21	7.97 <sup>2</sup>	556 ± 57	5.53 ± 0.32	3.67 ± 0.22
		(37.9, 37.9), n=7	(25.9, 27.0), n=1691	(2629, 2659), n=17	(2310, 2338), n=1691	(7.94, 8.00), n=1691	(513, 597), n=1691	(5.31, 5.75), n=1691	(3.53, 3.82), n=1691
Experimental tanks	Present day	37.8 ± 0.5	22.6 ± 1.9	2542 ± 54	2206 ± 63	8.06 ± 0.06	415 ± 70	5.65 ± 0.69	3.71 ± 0.46
		(37.3, 38.3), n=25	(20.7, 24.5), n=347	(2488, 2596), n=347	(2143, 2269), n=347	(8.00, 8.12), n=347	(345, 485), n=347	(4.96, 6.34), n=347	(3.25, 4.17), n=347
Experimental tanks	Low pH	37.8 ± 0.5	22.7 ± 1.9	2542 ± 54	2389 ± 65	7.73 ± 0.09	1048 ± 237	2.99 ± 0.56	1.97 ± 0.37
		(37.3, 38.3), n=25	(20.8, 24.6), n=348	(2488, 2596), n=348	(2324, 2454), n=348	(7.64, 7.82), n=348	(811, 1285), n=348	(2.43, 3.55), n=348	(1.60, 2.34), n=348

366 Experimental conditions

367 Weekly temperature in the tanks varied according to natural changes in the summer  
368 temperature profile at 10 m depth in Ischia, from  $19.08 \pm 0.06$  °C at the end of May 2019  
369 (mean  $\pm$  SE, n = 24) to  $21.51 \pm 0.07$  °C at the beginning of December (mean  $\pm$  SE, n = 24)  
370 with a maximum value of  $25.17 \pm 0.15$  °C in August (mean  $\pm$  SE, n = 24, Fig. S2  
371 Supplementary materials). The “present-day” treatment was maintained at a mean pH<sub>T</sub> of  $8.06$   
372  $\pm 0.06$  (n = 347) whereas “low pH” treatment had a pH<sub>T</sub> of  $7.73 \pm 0.09$  (n = 348). Salinity was  
373  $37.8 \pm 0.5$  (n = 25).

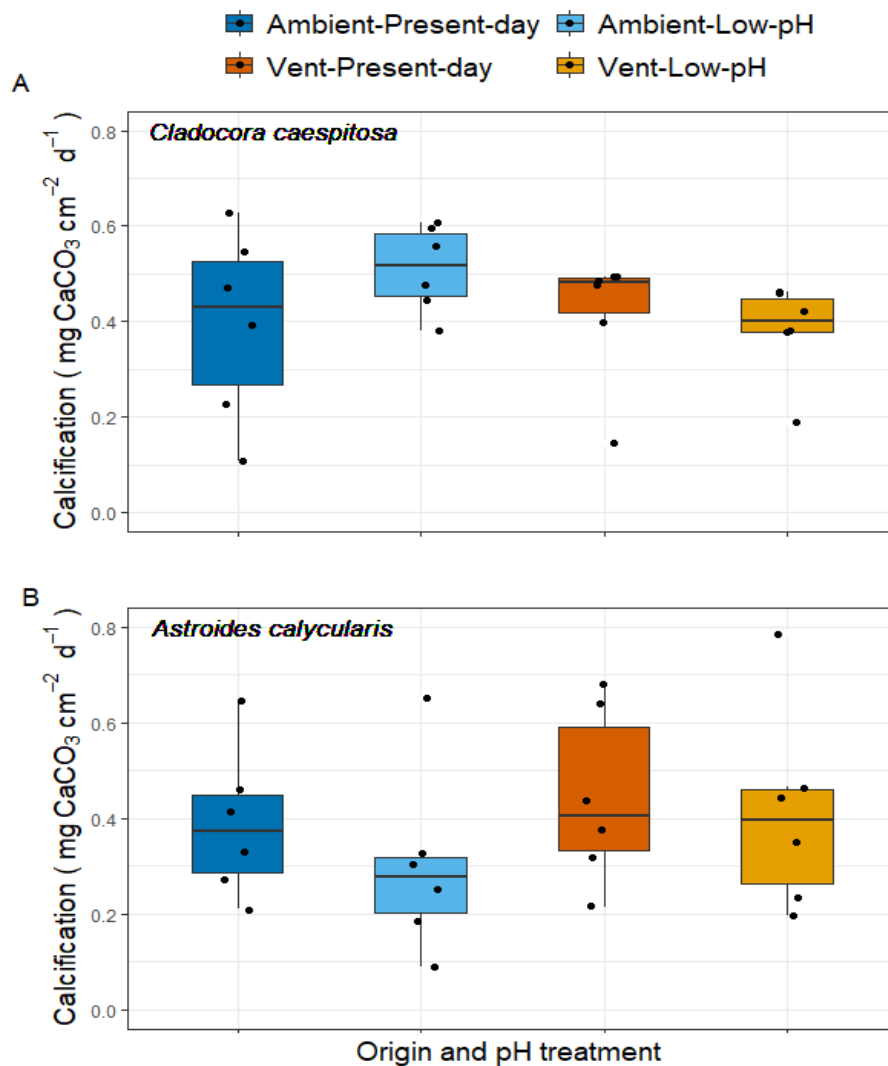
374 Colonies of *Astroides calycularis* had physical differences depending on their site of origin.  
375 85% (23/27 colonies) of vent and 14% (2/14 colonies) of ambient colonies did not present  
376 coenosarc (i.e. tissue between polyps). Furthermore, by comparing photos from the beginning  
377 and end of the experiment, it was observed that none of the *A. calycularis* colonies from  
378 ambient suffered polyp death, while three vent colonies showed 2/5, 1/7 and 4/9 dead polyps  
379 (number of dead polyps / total number of polyps in the colony). No polyp loss was observed  
380 in *Cladocora caespitosa*.

381 Six-month, monthly and short-term calcification rates

382 The rates of six-month calcification of *C. caespitosa* and *A. calycularis* were not affected by  
383 the origin and the pH treatment (Fig. 2; Tab. S3 Supplementary materials; Two-way ANOVA,  
384  $F_{1,20} = 1.778$ ,  $P = 0.2$  for *C. caespitosa*,  $F_{1,20} = 0.13$ ,  $P = 0.72$  for *A. calycularis*).

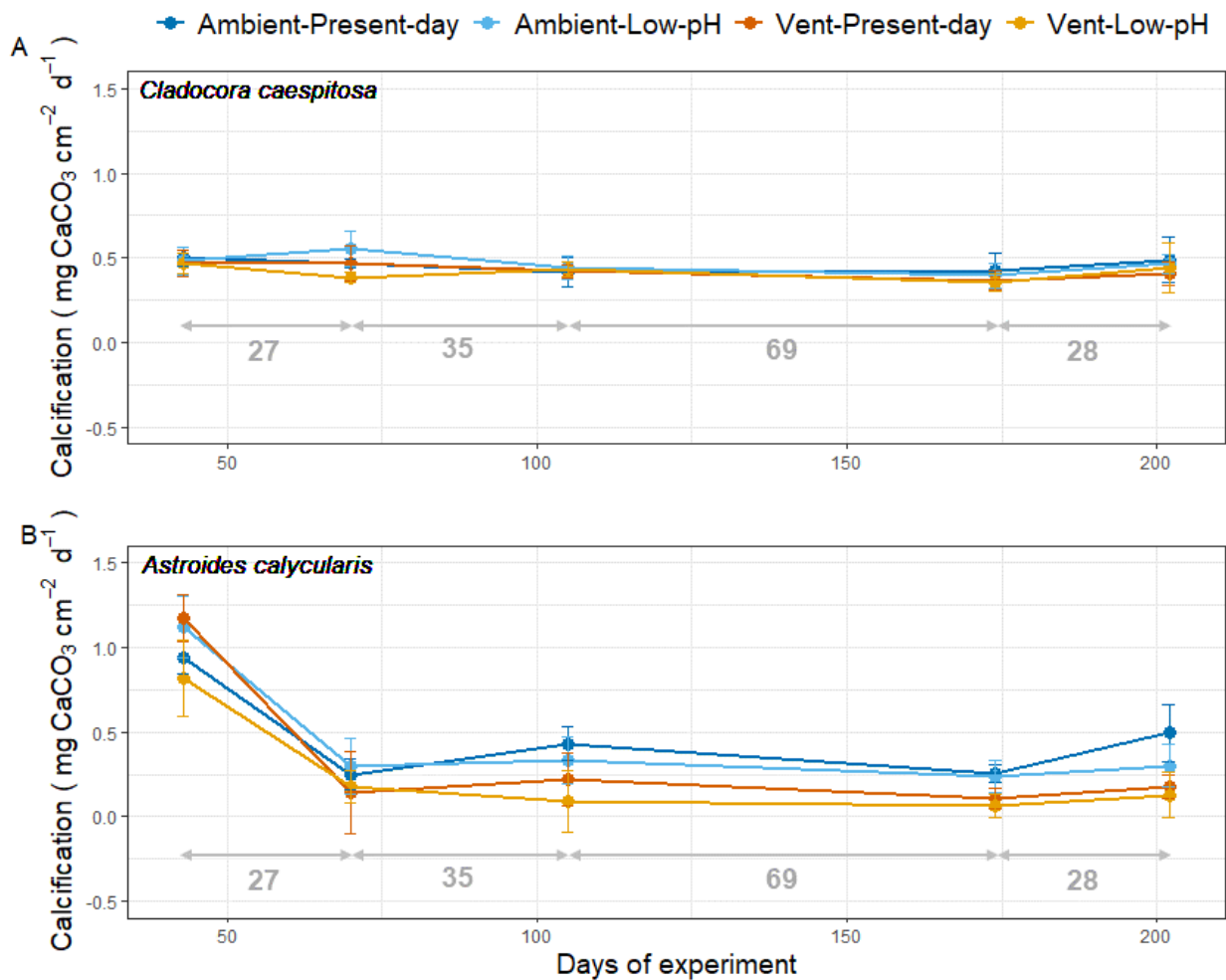
385 No statistically significant effect of origin and pH treatment on calcification rate was found in  
386 *C. caespitosa* over time (Fig. 3A;  $F_{1,110} = 1.919$ ,  $P = 0.17$ ). However, different calcification  
387 rates with time were found for *A. calycularis* (Fig. 3B,  $F_{1,112} = 26.2$ ,  $P < 0.001$ ), with  
388 significantly higher calcification measured during the first month of the experiment ( $1.0 \pm 0.2$

389 mg CaCO<sub>3</sub> cm<sup>-2</sup> d<sup>-1</sup>). The mean monthly calcification rate was 0.2 ± 0.1 mg CaCO<sub>3</sub> cm<sup>-2</sup> d<sup>-1</sup>  
390 during the following months of experiment.



391

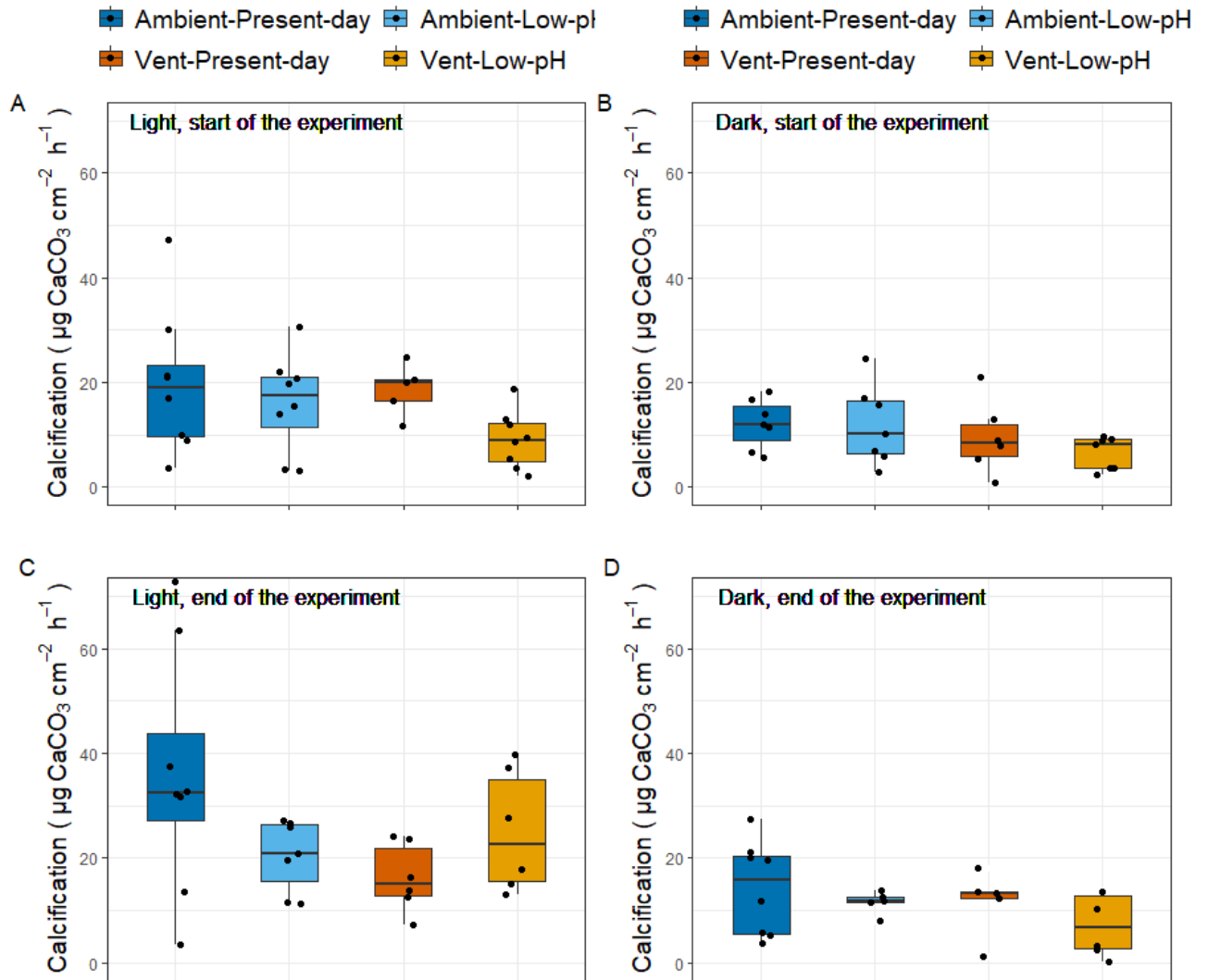
392 **Figure 2. Six-month calcification rates of *C. caespitosa* and *A. calycularis* collected from**  
393 **vent and ambient sites exposed to the two pH treatments (pHT = 8.08 ± 0.01, present**  
394 **day; pHT = 7.72 ± 0.01, low pH) during the entire duration of the experiment (202 days).**  
395 Panel A) shows *Cladocora caespitosa* and panel B) shows *Astroides calycularis*. Dots  
396 represent the mean calcification rates of colonies per experimental tank and boxes represent  
397 the median and the 25 and 75% quartiles. The color of the box indicates the origin and the  
398 treatment. n = 6 per pH treatment and origin.



399

400 **Figure 3. Calcification rates of *C. caespitosa* and *A. calycularis* from vent and ambient**  
 401 **sites under the two pH treatments (pH<sub>T</sub> = 8.08 ± 0.01, present day; pH<sub>T</sub> = 7.72 ± 0.01, low**  
 402 **pH) over time (every 27 to 35 days). Values are means ± SE, Panel A) *Cladocora caespitosa***  
 403 **and B) *Astroides calycularis*. The color of the dots and lines indicates the origin and the**  
 404 **treatment. We had a technical problem with day 139 weighing which is therefore not**  
 405 **represented here. Numbers below arrows between dots represent the number of days between**  
 406 **measurements. n = 6 per pH treatment and origin.**

407 Short-term calcification of *C. caespitosa* in the dark and in the light was not significantly  
 408 different at the start (Fig. 4A and 4B; 10 ± 1.1 and 15.65 ± 1.85 μg CaCO<sub>3</sub> cm<sup>-2</sup> h<sup>-1</sup>,  
 409 respectively) and the end of the experiment (Fig. 4C and 4D; 11.42 ± 1.40 and 25.21 ± 3.03  
 410 μg CaCO<sub>3</sub> cm<sup>-2</sup> h<sup>-1</sup>, respectively). Colonies light and dark calcification were also not affected  
 411 by origin and pH treatment (Fig. 4;  $F_{1,40} = 0.07$ ,  $P = 0.795$ ).



412

413 **Figure 4. Short-term calcification rates for *Cladocora caespitosa* from vent and ambient**  
 414 **sites under the two pH treatments (pH<sub>T</sub> = 8.08 ± 0.01, present day; pH<sub>T</sub> = 7.72 ± 0.01, low**  
 415 **pH) in the light and dark at the start (27<sup>th</sup> of June 2019) and end of the experiment (24<sup>th</sup>**  
 416 **of October 2019). Values are means ± SE. Rates were calculated using alkalinity anomaly**  
 417 **method following short term incubations (< 1 h) at 20°C. Panel A) and C) under light**  
 418 **conditions, B) and D) under dark conditions. Dots represent the calcification rates of the coral**  
 419 **colonies and boxes represent median and 25 and 75% quartiles. The color of the box indicates**  
 420 **the origin and the treatment. n = 5 to 8 per pH treatment and origin.**

421

422 Dark respiration and gross and net photosynthesis

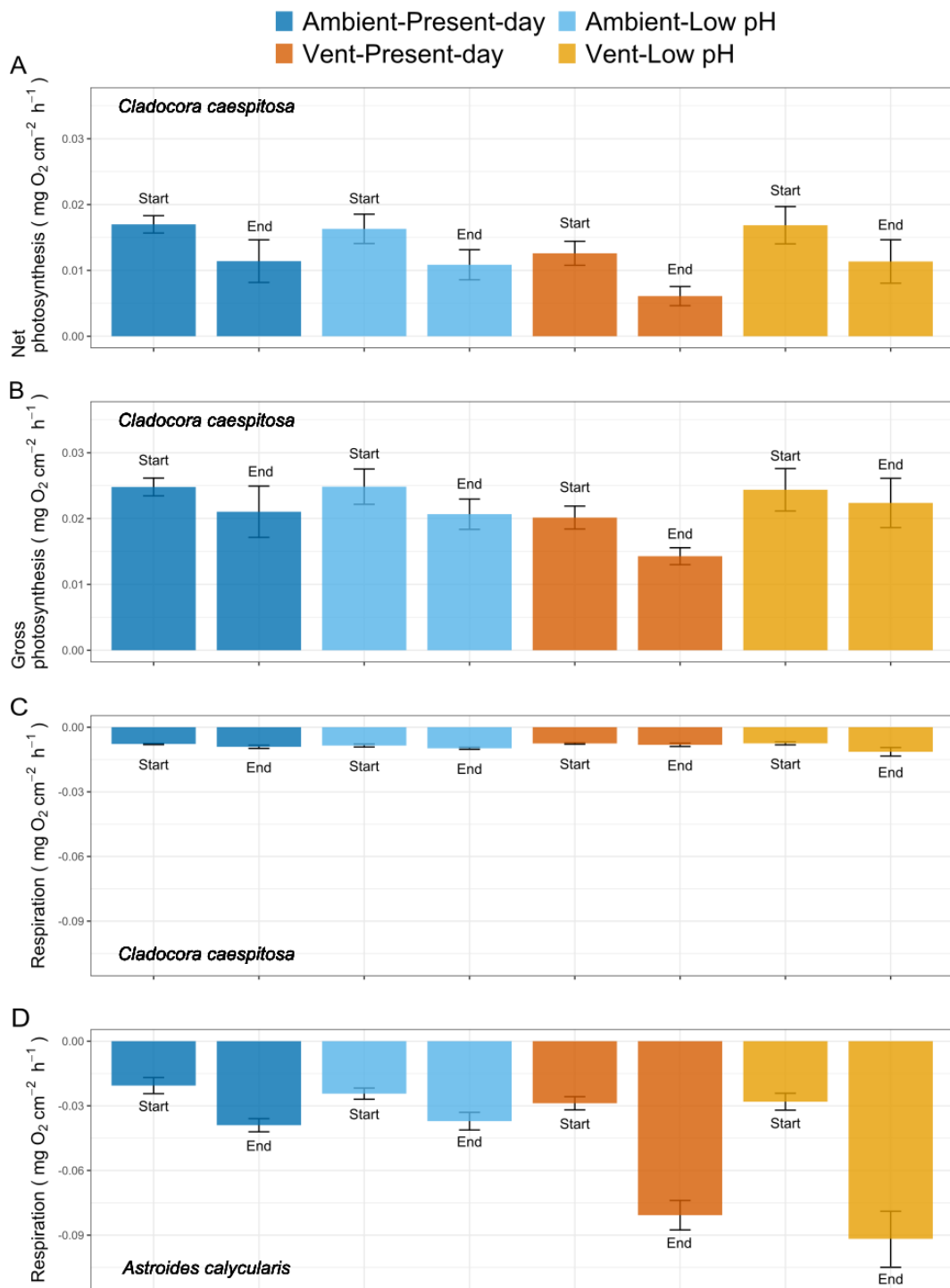
423 Net photosynthesis of *C. caespitosa* was not affected by origin and pH treatment (Fig. 5A;

424  $F_{1,40} = 2.36, P = 0.134$  and  $F_{1,40} = 1.24, P = 0.272$ , respectively), but was different between the

425 beginning and the end of the experiment (Fig. 5A;  $F_{1,40} = 13.14$ ,  $P < 0.001$ ). Gross  
426 photosynthesis of *C. caespitosa* did not exhibit any statistically significant difference between  
427 origin, pH treatment and time (Fig. 5B;  $F_{1,24} = 0.17$ ,  $P = 0.683$ ). Mean gross photosynthesis  
428 for all pH treatments was similar at the start and end of the experiment ( $0.024 \pm 0.001$  vs  
429  $0.020 \pm 0.002$  mg O<sub>2</sub> cm<sup>-2</sup> h<sup>-1</sup>, n = 30). As light and dark respiration may differ, gross  
430 photosynthesis measurements are uncertain, and most likely underestimated.

431 Dark respiration rate of *C. caespitosa* was not significantly different between origin and pH  
432 treatment (Fig. 5C,  $F_{1,24} = 0.008$ ,  $P = 0.93$  and  $F_{1,24} = 3.09$ ,  $P = 0.091$ , respectively), but was  
433 significantly different between the beginning and end of the experiment ( $F_{1,24} = 9.45$ ,  $P =$   
434  $0.005$ ). In June, mean dark respiration rates for all conditions (origin and pH treatment) was  
435  $-0.0079 \pm 0.0003$  mg O<sub>2</sub> cm<sup>-2</sup> h<sup>-1</sup> (n = 30) while in November it was  $-0.0097 \pm 0.0006$  mg O<sub>2</sub>  
436 cm<sup>-2</sup> h<sup>-1</sup> (n = 28), which represents a 23% of increase in dark respiration.

437 At the start of the experiment, the dark respiration of *A. calycularis* did not differ between  
438 origin or pH treatment (Fig. 5D,  $F_{1,37} = 0.32$ ,  $P = 0.58$ ). At the end of the experiment (Fig.  
439 5D), a significant difference between site of origin was observed ( $F_{1,36} = 18.5$ ,  $P < 0.0001$ ),  
440 with corals from the ambient site having a mean dark respiration of  $-0.038 \pm 0.003$  mg O<sub>2</sub> cm<sup>-2</sup>  
441 h<sup>-1</sup> (n = 13) whilst colonies from the CO<sub>2</sub> vent site had a rate of  $-0.087 \pm 0.008$  mg O<sub>2</sub> cm<sup>-2</sup> h<sup>-1</sup>  
442 (n = 27). The overall (all treatments) mean dark respiration rate were also different at the  
443 start and at the end of the experiment, with a lower mean dark respiration at the start ( $-0.026 \pm$   
444  $0.002$  vs  $-0.071 \pm 0.007$  mg O<sub>2</sub> cm<sup>-2</sup> h<sup>-1</sup>;  $F_{1,36} = 52.3$ ,  $P < 0.0001$ ).



445

446 **Figure 5. Net and gross photosynthesis and dark respiration rates of *C. caespitosa* and *A.***  
 447 ***calycularis* from the vent and ambient sites under the two pH treatments (pH<sub>T</sub> = 8.08 ±**  
 448 **0.01, present day; pH<sub>T</sub> = 7.72 ± 0.01, low pH) at the start (27<sup>th</sup> of June 2019) and end of the**  
 449 **experiment (24<sup>th</sup> of October 2019). Values are means ± SE, Panel A) *Cladocora***  
 450 ***caespitosa*'s net photosynthesis, B) *Cladocora caespitosa*'s gross photosynthesis, C)**  
 451 ***Cladocora caespitosa*'s dark respiration. D) *Astroides calycularis*' dark respiration. The color**  
 452 **of the bars indicates the origin and the treatment. n = 6 to 15 per pH treatment and origin.**

453 **Discussion**

454 During this six-month laboratory experiment, we tested whether colonies of the  
455 zooxanthellate coral *Cladocora caespitosa* and the azooxanthellate coral *Astroides calycularis*  
456 growing in naturally acidified waters were more tolerant to low pH than colonies from  
457 ambient pH sites or acclimated. In contrast to our initial hypothesis, calcification rates and  
458 metabolic responses did not change for any coral species no matter the site of origin and pH  
459 treatment. Therefore, our results suggest that both species, independently of environmental  
460 history and trophic strategy, can tolerate low pH conditions for six months, under controlled  
461 conditions in aquaria. In contrast, in situ surveys revealed lower abundance and smaller sizes  
462 for both corals at CO<sub>2</sub> vent sites compared with ambient sites.

463 The hypothesis that corals from vent sites would be less impacted by low pH stems from  
464 reports that organisms experiencing highly variable or low pH in their natural habitat may be  
465 more tolerant to ocean acidification (Cornwall et al. 2018). Corals living in suboptimal  
466 environmental conditions may possess physiological and potentially genetic mechanisms that  
467 confer tolerance to such environmental conditions (Camp et al 2018, Teixidó et al 2020). For  
468 example, microhabitats experiencing periodic temperature extremes are potential habitats for  
469 heat tolerant corals (Schoepf et al. 2015), yet these habitats can exhibit a mosaic of  
470 populations, harboring species previously reported with high to low thermal tolerance  
471 (Ainsworth et al. 2016). Such physiological mechanisms and intraspecific variability may  
472 exist in *C. caespitosa* and *A. calycularis* which highlights the importance of studying the  
473 influence of suboptimal environmental conditions on tolerance to stressors.

474 Previous research has shown a decrease in calcification when corals were transplanted from  
475 ambient pH sites to CO<sub>2</sub> vents (Rodolfo-Metalpa et al. 2011; Prada et al. 2017). However,  
476 previous studies on temperate/cold-water coral including *C. caespitosa* and *A. calycularis*  
477 have also shown a greater tolerance to ocean acidification than most tropical corals (see Tab.

478 S5 Supplementary materials). Calcification rates reported in the present study agree with  
479 earlier studies. For *C. caespitosa*, Rodolfo-Metalpa et al. (2010) observed a yearly  
480 calcification rate of  $0.51 \text{ mg CaCO}_3 \text{ cm}^{-2} \text{ d}^{-1}$ , which is similar to what we measured during  
481 this six-month experiment ( $0.43 \pm 0.03 \text{ mg CaCO}_3 \text{ cm}^{-2} \text{ d}^{-1}$ ). The calcification rates of *A.*  
482 *calycularis* measured here are also of the same order of magnitude to those reported by  
483 Movilla et al. (2016) ( $0.39 \pm 0.04$  and  $0.47 \pm 0.06 \text{ mg CaCO}_3 \text{ cm}^{-2} \text{ d}^{-1}$ , respectively). In  
484 contrast to temperate and cold-water corals, tropical corals tend to be more affected by ocean  
485 acidification, as they exhibit a mean decrease in calcification of 10-25% when exposed to the  
486  $\text{pCO}_2$  expected by the end of the century under the high- $\text{CO}_2$  emissions scenario (Chan and  
487 Connolly 2013; Cornwall et al. 2021). Most tropical corals investigated so far are fast  
488 calcifiers, growing in warm waters, therefore as seawater pH declines, they may be unable to  
489 maintain these energetically costly fast rates of calcification (Comeau et al. 2014). In contrast,  
490 temperate and cold-water corals are slower calcifiers with lower energy requirements for  
491 mineralization, thus making them more likely to maintain constant calcification rates at lower  
492 pH (Rodolfo-Metalpa et al. 2010, Comeau et al. 2014). Ries et al. (2010), also suggested that  
493 the effect of acidification on the calcification of temperate corals, such as *Oculina arbuscula*,  
494 may manifest at a lower pH threshold compared to tropical corals. The capacity of *C.*  
495 *caespitosa* and *A. calycularis* to control the carbonate chemistry at their site of calcification  
496 could explain this tolerance to low pH. For example, using the geochemical proxy  $\delta^{11}\text{B}$  it was  
497 shown that the temperate coral *Balanophyllia europaea* at the  $\text{CO}_2$  vents of Panarea Island  
498 (Italy) can maintain constant calcifying fluid pH when exposed to pH ranging from 8.07 to  
499 7.74 (Wall et al. 2019). This confirms the capacity of some corals to maintain internal pH  
500 homeostasis and utilize this as a way of calcifying under reduced seawater pH (Comeau et al.  
501 2019).

502 From this study no conclusions can be drawn as to whether colonies from the vent sites are  
503 acclimated to low pH, as colonies from both vent sites and the ambient sites were not affected  
504 by low pH in the laboratory. However, controlling the transport of calcium and inorganic  
505 carbon to the calcifying medium and producing the skeletal organic matrix are all energy-  
506 demanding processes (Allemand et al. 2011, Wall et al. 2019), therefore the maintenance of  
507 calcification rates under these treatments may have come at a cost. For example, Wall et al.  
508 (2019) suggest that the inactivation of some calciblastic cells could compensate for the  
509 energy required to regulate internal pH and maintain calcification rates under low seawater  
510 pH, but at the cost of increased skeletal porosity. This is supported by a study that showed a  
511 constant growth rate of the temperate coral *B. europaea* in acidified conditions at the expense  
512 of skeletal density (Fantazzini et al. 2015), which in return increases the sensitivity to  
513 bioerosion and susceptibility to damage (Crook et al. 2013). Skeletal porosity was not  
514 measured in the present study. However, increased sensitivity to bioerosion can also be linked  
515 to the tissue coverage of the skeleton. Rodolfo-Metalpa et al. (2010) observed that following  
516 transplantation to low pH conditions, skeleton dissolution was observed in *Cladocora*  
517 *caespitosa* which had exposed skeleton, and not in *Balanophyllia europaea* which had less  
518 exposed skeleton. In our study, we observed that most of the *A. calycularis* colonies collected  
519 at the CO<sub>2</sub> vent sites did not possess coenosarc (i.e. coral tissue between polyps) and exhibited  
520 polyp death during our experiment. These phenomena were also observed in natural colonies  
521 of *A. calycularis* (Teixidó et al. 2020) and the corals *Pocillopora damicornis* and *Oculina*  
522 *patagonica* when incubated at low pH (Kvitt et al. 2015). The increased sensitivity to  
523 bioerosion of *A. calycularis* and *C. caespitosa* with exposed skeleton could explain in part the  
524 field observation.

525 Field observations confirmed the difference between the population of the CO<sub>2</sub> vent and  
526 ambient sites, as both corals were less abundant and had smaller colonies at the vent sites

527 (Fig. S3 Supplementary materials, Teixidó et al. 2020). These contrasting results between  
528 field and laboratory observations, could be explained by differences in pH variability, which  
529 is much greater in the field with short periods of very low pH. Alternatively, other  
530 environmental parameters such as food availability or biological interactions (e.g.,  
531 competition with algae) may contribute to these differences. pH variability at the CO<sub>2</sub> vent  
532 sites can be very high, as pH<sub>T</sub> can range from 6.70 to 8.13 in a day (Foo et al. 2018, Teixidó et  
533 al. 2020), whereas pH<sub>T</sub> was very stable during our pH-controlled laboratory experiment (pH<sub>T</sub>  
534 = 7.72 ± 0.01 for low pH treatment). It may be that no differences in calcification and  
535 photosynthesis were observed in the laboratory, due to the fact that both corals are slow-  
536 growing and long-lived species that have had a lifetime to acclimatize to their environmental  
537 pH. Therefore, the six-month time scale of the experiment may not have been enough to  
538 trigger any visible variation. However, even if our results did not show any statistical  
539 difference between treatments during the laboratory experiment, different trends in  
540 calcification between conditions can be observed for *A. calycularis*. The colonies from  
541 ambient-low pH condition seem to have lower calcification rate than the control colonies of  
542 ambient-present day condition (Fig. 2), suggesting a possible impact of low pH on  
543 calcification in the short term. The same trend is observed with the colonies from the vent  
544 site, as the vent-low pH presents reduced calcification rate compared to the vent-present day  
545 condition. Moreover, calcification was similar in the vent-low pH and the control ambient-  
546 present day conditions. This trend suggests a possible acclimation to low pH in corals  
547 growing at the CO<sub>2</sub> vent site

548 Zooxanthellate and azooxanthellate corals were both used in the present study to assess the  
549 role that photosynthesis could play in mitigating the effects of ocean acidification on  
550 calcification. In zooxanthellate corals, light-enhanced calcification describes the relationship  
551 between calcification, photosynthesis and irradiance (Gattuso et al. 1999; Allemand et al.

2011). Four main mechanisms explaining light-enhanced calcification were proposed: photosynthesis could (1) supply energy to the animal through the translocation of photosynthates, (2) increase pH at the site of calcification by using CO<sub>2</sub>, (3) remove phosphate, which is poison to carbonate crystallization, and (4) facilitate the production of the organic matrix which serves as a scaffold in which CaCO<sub>3</sub> is precipitated (Allemand et al. 2011). Here, short-term calcification of *C. caespitosa* was higher in light than in the dark, with a mean light:dark calcification ratio of 2.38 (See Tab. S4 Supplementary materials), which is close to the mean ratio of 3.0 obtained by Gattuso et al. (1999). However, neither light nor dark calcification rates differed with experimental pH conditions, thus we cannot conclude that photosynthesis did provide better tolerance to ocean acidification. Furthermore, no difference in the response of calcification to ocean acidification was observed between the zooxanthellate (*C. caespitosa*) and azooxanthellate species (*A. calycularis*). The data from the in situ survey at Ischia did not highlight a difference between the zooxanthellate and azooxanthellate corals either, as the size and abundance of colonies from CO<sub>2</sub> vent sites were lower for both species. Contrastingly, Prada et al. (2017) reported that the zooxanthellate coral *B. europaea* was unaffected by low pH conditions, whereas the azooxanthellate corals *Leptopsammia pruvoti* and *A. calycularis* showed a negative effect of pH on calcification. However, the study of Prada et al. (2017) was conducted in situ, on corals transplanted next to CO<sub>2</sub> vents in Panarea Island, whereas our study is based on a laboratory experiment and field observations. Feeding could also explain this difference as it can mitigate the negative effects of environmental stressors on coral physiology (Fox et al. 2018). In our experiment, corals were fed freshly hatched *Artemia nauplii* three-times a week therefore the demand of energy required to maintain calcification under low pH was likely sustained by heterotrophy (Edmunds 2011). Kornder et al. (2018) showed that in studies where corals were fed, the negative impacts of ocean acidification on corals were mitigated. Therefore, the fact that

577 Movilla et al. (2012) observed a decrease in calcification at low pH in *C. caespitosa* may be  
578 explained by the fact that the colonies were only fed once per week.

579 No difference in photosynthesis was observed between site of origin or pH treatment. This  
580 aligns with the observation that there is a limited impact of environmentally relevant  
581 decreases in pH on photosynthesis (Comeau et al. 2017), and that low pH rarely causes  
582 bleaching (Anthony et al. 2008). Moreover, Mediterranean corals harbor Clade B  
583 *Symbiodinium*, that have growth rates, photosynthetic capacities and respiration rates that are  
584 unaffected by acidification (Brading et al. 2011). Respiration was also not affected by the pH  
585 treatment in *C. caespitosa*, confirming previous observations for this species (Rodolfo-  
586 Metalpa et al. 2010), and other coral species (Comeau et al. 2017). However, colonies of *A.*  
587 *calycularis* from the vent site exhibited a higher rate of respiration at the end of the  
588 experiment (November) for both low and present-day pH treatments. This result contrasts  
589 with studies that show a decrease in respiration at lower pH (e.g. Comeau et al. 2014), or no  
590 impact on respiration (Rodolfo-Metalpa et al. 2010; Comeau et al. 2017). However, an  
591 increase in respiration could be due to the increased energetic demand associated with  
592 maintaining calcification rates at lower pH (Comeau et al. 2017). For example, a decrease in  
593 seawater  $pH_T$  of 0.7 units requires an additional  $1-2 \text{ kJ of energy mol}^{-1}$  of  $\text{CaCO}_3$   
594 precipitated (McCulloch et al. 2012a). For zooxanthellate corals, this energy is less than 1%  
595 of the energy provided by photosynthesis, however, for azooxanthellate corals such as *A.*  
596 *calycularis*, respiration is the only way to up-regulate this energy demand. Moreover, the  
597 increase of respiration from colonies of vent sites of *A. calycularis* could be partly due to the  
598 smaller size of colonies at the vent site than at the ambient site (Edmunds and Burgess 2016).

599 Although the corals studied here showed tolerance in the laboratory to pH conditions expected  
600 by 2100, it is a fragile equilibrium that can be disrupted by the inclusion of changes in other

601 environmental variables such as temperature that could lead to a greater impact on  
602 physiological processes and survival, as observed in the in situ survey and predicted by the  
603 negative trend on the calcification of *A. calycularis*. For example, marine heatwaves can lead  
604 to mass mortality of *C. caespitosa* and *A. calycularis* (Rodolfo-Metalpa et al. 2005) and are  
605 projected to be more frequent and severe in the future (Galli et al. 2017, Smale et al. 2019).  
606 Moreover, the impact of ocean acidification on reproduction as well as larval and juvenile  
607 survival, which can limit the persistence and dispersion of a species remains to be  
608 investigated. The present study contributes to our knowledge of *Cladocora caespitosa* and  
609 *Astroides calycularis*' ability to survive under future ocean acidification conditions. Such  
610 information will improve our ability to manage and conserve the biodiversity of  
611 Mediterranean calcifying species.

612

613

614

615

616

617

618

619

620

621

622

623 **References**

- 624 Ainsworth, T. D., S. F. Heron, J. C. Ortiz, P. J. Mumby, A. Grech, D. Ogawa, C. M. Eakin,  
625 and W. Leggat. 2016. Climate change disables coral bleaching protection on the Great  
626 Barrier Reef. *Science*. **352**: 338–342. doi:10.1126/science.aac7125
- 627 Allemand, D., É. Tambutté, D. Zoccola, and S. Tambutté. 2011. Coral Calcification, Cells to  
628 Reefs, p. 119–150. *In* Z. Dubinsky and N. Stambler [eds.], *Coral Reefs: An Ecosystem in*  
629 *Transition*. Springer Netherlands.
- 630 Anthony, K. R. N., D. I. Kline, G. Diaz-Pulido, S. Dove, and O. Hoegh-Guldberg. 2008.  
631 Ocean acidification causes bleaching and productivity loss in coral reef builders. *Proc.*  
632 *Natl. Acad. Sci.* **105**: 17442–17446. doi:10.1073/pnas.0804478105
- 633 Brading, P., M. E. Warner, P. Davey, D. J. Smith, E. P. Achterberg, and D. J. Suggett. 2011.  
634 Differential effects of ocean acidification on growth and photosynthesis among  
635 phlotypes of *Symbiodinium* (Dinophyceae). *Limnol. Oceanogr.* **56**: 927–938.  
636 doi:10.4319/lo.2011.56.3.0927
- 637 Caldeira, K., and M. E. Wickett. 2003. Anthropogenic carbon and ocean pH. *Nature* **425**:  
638 365–365. doi:10.1038/425365a
- 639 Camp, E. F., V. Schoepf, P. J. Mumby, L. A. Hardtke, R. Rodolfo-Metalpa, D. J. Smith, and  
640 D. J. Suggett. 2018. The future of coral reefs subject to rapid climate change: lessons  
641 from natural extreme environments. *Front. Mar. Sci.* **5**: 1–21.  
642 doi:10.3389/fmars.2018.00004
- 643 Chan, N. C. S., and S. R. Connolly. 2013. Sensitivity of coral calcification to ocean  
644 acidification: a meta-analysis. *Glob. Chang. Biol.* **19**: 282–290. doi:10.1111/gcb.12011
- 645 Comeau, S., C. E. Cornwall, T. M. DeCarlo, S. S. Doo, R. C. Carpenter, and M. T.

646 McCulloch. 2019. Resistance to ocean acidification in coral reef taxa is not gained by  
647 acclimatization. *Nat. Clim. Chang.* **9**: 477–483. doi:10.1038/s41558-019-0486-9

648 Comeau, S., R. C. Carpenter, and P. J. Edmunds. 2017. Effects of  $p\text{CO}_2$  on photosynthesis  
649 and respiration of tropical scleractinian corals and calcified algae. *ICES J. Mar. Sci.* **74**:  
650 1092–1102. doi:10.1093/icesjms/fsv267

651 Comeau, S., P. J. Edmunds, N. B. Spindel, and R. C. Carpenter. 2014. Fast coral reef  
652 calcifiers are more sensitive to ocean acidification in short-term laboratory incubations.  
653 *Limnol. Oceanogr.* **59**: 1081–1091. doi:10.4319/lo.2014.59.3.1081

654 Cornwall, C. E., S. Comeau, N. A. Kornder, and others. 2021. Global declines in coral reef  
655 calcium carbonate production under ocean acidification and warming. *Proc. Natl. Acad.*  
656 *Sci.* **118**: e2015265118. doi:10.1073/pnas.2015265118

657 Cornwall, C. E., and others. 2020. A coralline alga gains tolerance to ocean acidification over  
658 multiple generations of exposure. *Nat. Clim. Chang.* **10**: 143–146. doi:10.1038/s41558-  
659 019-0681-8

660 Cornwall, C. E., S. Comeau, T. M. DeCarlo, B. Moore, Q. D’Alexis, and M. T. McCulloch.  
661 2018. Resistance of corals and coralline algae to ocean acidification: Physiological  
662 control of calcification under natural pH variability. *Proc. R. Soc. B Biol. Sci.* **285**.  
663 doi:10.1098/rspb.2018.1168

664 Crook, E. D., A. L. Cohen, M. Rebolledo-Vieyra, L. Hernandez, and A. Paytan. 2013.  
665 Reduced calcification and lack of acclimatization by coral colonies growing in areas of  
666 persistent natural acidification. *Proc. Natl. Acad. Sci.* **110**: 11044–11049.  
667 doi:10.1073/pnas.1301589110

668 Davies, S. P. 1989. Short-term growth measurements of corals using an accurate buoyant  
669 weighing technique. *Mar. Biol.* **101**: 389–395. doi:10.1007/BF00428135

670 Davy, S. K., D. Allemand, and V. M. Weis. 2012. Cell biology of cnidarian-dinoflagellate  
671 symbiosis. *Microbiol. Mol. Biol. Rev.* **76**: 229–261. doi:10.1128/MMBR.05014-11

672 Dickson, A. G., C. L. Sabine, and J. R. Christian. 2007. SOP 3a Determination of total  
673 alkalinity in sea water using an open-cell titration, p. 191. *In* Guide to best practices for  
674 ocean CO<sub>2</sub> measurements. North Pacific Marine Science Organization.

675 Edmunds, P., and R. Gates. 2008. Acclimatization in tropical reef corals. *Mar. Ecol. Prog.*  
676 *Ser.* **361**: 307–310. doi:10.3354/meps07556

677 Edmunds, P. J. 2011. Zooplanktivory ameliorates the effects of ocean acidification on the reef  
678 coral *Porites* spp. *Limnol. Oceanogr.* **56**: 2402–2410. doi:10.4319/lo.2011.56.6.2402

679 Edmunds, P. J., and S. C. Burgess. 2016. Size-dependent physiological responses of the  
680 branching coral *Pocillopora verrucosa* to elevated temperature and pCO<sub>2</sub>. *J. Exp. Biol.*  
681 **219**: 3896–3906. doi:10.1242/jeb.146381

682 Erez, J., S. Reynaud, J. Silverman, K. Schneider, and D. Allemand. 2011. Coral calcification  
683 under ocean acidification and global change, p. 151–176. *In* Z. Dubinsky and N.  
684 Stambler [eds.], *Coral Reefs: An Ecosystem in Transition*. Springer Netherlands.

685 Fabricius, K. E., and others. 2011. Losers and winners in coral reefs acclimatized to elevated  
686 carbon dioxide concentrations. *Nat. Clim. Chang.* **1**: 165–169. doi:10.1038/nclimate1122

687 Fantazzini, P., and others. 2015. Gains and losses of coral skeletal porosity changes with  
688 ocean acidification acclimation. *Nat. Commun.* **6**: 7785. doi:10.1038/ncomms8785

689 Foo, S. A., M. Byrne, E. Ricevuto, and M. C. Gambi. 2018. The carbon dioxide vents of  
690 Ischia, Italy, a natural system to assess impacts of ocean acidification on marine  
691 ecosystems: an overview of research and comparisons with other vent systems, p. 237–  
692 310. *In* S.J. Hawkins, A.J. Evans, A.C. Dale, L.B. Firth, and I.P. Smith [eds.],

693 Oceanography and Marine Biology. CRC Press.

694 Foster, T., and P. L. Clode. 2016. Skeletal mineralogy of coral recruits under high temperature  
695 and  $p\text{CO}_2$ . *Biogeosciences* **13**: 1717–1722. doi:10.5194/bg-13-1717-2016

696 Fox, M. D., and others. 2018. Gradients in primary production predict trophic strategies of  
697 mixotrophic corals across spatial scales. *Curr. Biol.* **28**: 3355-3363.e4.  
698 doi:10.1016/j.cub.2018.08.057

699 Galli, G., C. Solidoro, and T. Lovato. 2017. Marine heat waves hazard 3D maps and the risk  
700 for low motility organisms in a warming Mediterranean Sea. *Front. Mar. Sci.* **4**: 1–14.  
701 doi:10.3389/fmars.2017.00136

702 Gattuso, J.-P., D. Allemand, and M. Frankignoulle. 1999. Photosynthesis and calcification at  
703 cellular, organismal and community levels in coral reefs: A review on interactions and  
704 control by carbonate chemistry. *Am. Zool.* **39**: 160–183. doi:10.1093/icb/39.1.160

705 Gattuso, J. -P., J.-M. Epitalon, H. Lavigne, and J. C. Orr. 2020. seacarb: seawater carbonate  
706 chemistry. R package version 3.2.13. <https://cran.r-project.org/package=seacarb>.

707 Gibbin, E. M., H. M. Putnam, S. K. Davy, and R. D. Gates. 2014. Intracellular pH and its  
708 response to  $\text{CO}_2$ -driven seawater acidification in symbiotic versus non-symbiotic coral  
709 cells. *J. Exp. Biol.* **217**: 1963–1969. doi:10.1242/jeb.099549

710 González-Delgado, S., and J. C. Hernández. 2018. The importance of natural acidified  
711 systems in the study of ocean acidification: what have we learned?, p. 57–99. *In*  
712 *Advances in Marine Biology*. Academic Press.

713 Gruber, N., and others. 2019. The oceanic sink for anthropogenic  $\text{CO}_2$  from 1994 to 2007.  
714 *Science* (80-. ). **363**: 1193–1199. doi:10.1126/science.aau5153

715 Hall-Spencer, J. M., and others. 2008. Volcanic carbon dioxide vents show ecosystem effects

716 of ocean acidification. *Nature* **454**: 96–99. doi:10.1038/nature07051

717 Inoue, M., T. Nakamura, Y. Tanaka, A. Suzuki, Y. Yokoyama, H. Kawahata, K. Sakai, and N.  
718 Gussone. 2018. A simple role of coral-algal symbiosis in coral calcification based on  
719 multiple geochemical tracers. *Geochim. Cosmochim. Acta* **235**: 76–88.  
720 doi:10.1016/j.gca.2018.05.016

721 Kersting, D.-K., and C. Linares. 2012. *Cladocora caespitosa* bioconstructions in the  
722 Columbretes Islands Marine Reserve (Spain, NW Mediterranean): distribution, size  
723 structure and growth. *Mar. Ecol.* **33**: 427–436. doi:10.1111/j.1439-0485.2011.00508.x

724 Kornder, N. A., B. M. Riegl, and J. Figueiredo. 2018. Thresholds and drivers of coral  
725 calcification responses to climate change. *Glob. Chang. Biol.* **24**: 5084–5095.  
726 doi:10.1111/gcb.14431

727 Kroeker, K. J., R. L. Kordas, R. Crim, I. E. Hendriks, L. Ramajo, G. S. Singh, C. M. Duarte,  
728 and J.-P. Gattuso. 2013a. Impacts of ocean acidification on marine organisms:  
729 quantifying sensitivities and interaction with warming. *Glob. Chang. Biol.* **19**: 1884–  
730 1896. doi:10.1111/gcb.12179

731 Kroeker, K. J., M. C. Gambi, and F. Micheli. 2013b. Community dynamics and ecosystem  
732 simplification in a high-CO<sub>2</sub> ocean. *Proc. Natl. Acad. Sci.* **110**: 12721–12726.  
733 doi:10.1073/pnas.1216464110

734 Kvitt, H., E. Kramarsky-Winter, K. Maor-Landaw, K. Zandbank, A. Kushmaro, H. Rosenfeld,  
735 M. Fine, and D. Tchernov. 2015. Breakdown of coral colonial form under reduced pH  
736 conditions is initiated in polyps and mediated through apoptosis. *Proc. Natl. Acad. Sci.*  
737 U. S. A. **112**: 2082–2086. doi:10.1073/pnas.1419621112

738 Linares, C., and others. 2015. Persistent natural acidification drives major distribution shifts in

739 marine benthic ecosystems. *Proc. R. Soc. B Biol. Sci.* **282**: 20150587.  
740 doi:10.1098/rspb.2015.0587

741 Marsh, J. A. J. 1970. Primary productivity of reef-building calcareous red algae. *Ecol. Soc.*  
742 *Am.* **51**: 255–263.

743 Martin, S., and J.-P. Gattuso. 2009. Response of Mediterranean coralline algae to ocean  
744 acidification and elevated temperature. *Glob. Chang. Biol.* **15**: 2089–2100.  
745 doi:10.1111/j.1365-2486.2009.01874.x

746 McCulloch, M., J. Falter, J. Trotter, and P. Montagna. 2012a. Coral resilience to ocean  
747 acidification and global warming through pH up-regulation. *Nat. Clim. Chang.* **2**: 623–  
748 627. doi:10.1038/nclimate1473

749 McCulloch, M., and others. 2012b. Resilience of cold-water scleractinian corals to ocean  
750 acidification: Boron isotopic systematics of pH and saturation state up-regulation.  
751 *Geochim. Cosmochim. Acta* **87**: 21–34. doi:10.1016/j.gca.2012.03.027

752 Movilla, J., E. Calvo, R. Coma, E. Serrano, À. López-Sanz, and C. Pelejero. 2016. Annual  
753 response of two Mediterranean azooxanthellate temperate corals to low-pH and high-  
754 temperature conditions. *Mar. Biol.* **163**: 135. doi:10.1007/s00227-016-2908-9

755 Movilla, J., E. Calvo, C. Pelejero, R. Coma, E. Serrano, P. Fernández-Vallejo, and M. Ribes.  
756 2012. Calcification reduction and recovery in native and non-native Mediterranean corals  
757 in response to ocean acidification. *J. Exp. Mar. Bio. Ecol.* **438**: 144–153.  
758 doi:10.1016/j.jembe.2012.09.014

759 Muller-Parker, G., C. F. D’Elia, and C. B. Cook. 2015. Interactions between corals and their  
760 symbiotic algae. *Coral Reefs Anthr.* 99–116. doi:10.1007/978-94-017-7249-5\_5

761 Ohki, S., and others. 2013. Calcification responses of symbiotic and aposymbiotic corals to

762 near-future levels of ocean acidification. *Biogeosciences* **10**: 6807–6814.  
763 doi:10.5194/bg-10-6807-2013

764 Orr, J. C., and others. 2005. Anthropogenic ocean acidification over the twenty-first century  
765 and its impact on calcifying organisms. *Nature* **437**: 681–686. doi:10.1038/nature04095

766 Peirano, A., C. Morri, C. N. Bianchi, and R. Rodolfo-Metalpa. 2001. Biomass, carbonate  
767 standing stock and production of the mediterranean coral *Cladocora caespitosa* (L.).  
768 *Facies* **44**: 75–80. doi:10.1007/BF02668168

769 Prada, F., and others. 2017. Ocean warming and acidification synergistically increase coral  
770 mortality. *Sci. Rep.* **7**: 1–10. doi:10.1038/srep40842

771 Ries, J. B., A. L. Cohen, and D. C. McCorkle. 2010. A nonlinear calcification response to  
772 CO<sub>2</sub>-induced ocean acidification by the coral *Oculina arbuscula*. *Coral Reefs* **29**: 661–  
773 674. doi:10.1007/s00338-010-0632-3

774 Rodolfo-Metalpa, R., and others. 2011. Coral and mollusc resistance to ocean acidification  
775 adversely affected by warming. *Nat. Clim. Chang.* **1**: 308–312.  
776 doi:10.1038/nclimate1200

777 Rodolfo-Metalpa, R., S. Martin, C. Ferrier-Pagès, and J. P. Gattuso. 2010. Response of the  
778 temperate coral *Cladocora caespitosa* to mid- and long-term exposure to *p*CO<sub>2</sub> and  
779 temperature levels projected for the year 2100 AD. *Biogeosciences* **7**: 289–300.  
780 doi:10.5194/bg-7-289-2010

781 Rodolfo-Metalpa, R., C. N. Bianchi, A. Peirano, and C. Morri. 2005. Tissue necrosis and  
782 mortality of the temperate coral *Cladocora caespitosa*. *Ital. J. Zool.* **72**: 271–276.  
783 doi:10.1080/11250000509356685

784 Savolainen, O., M. Lascoux, and J. Merilä. 2013. Ecological genomics of local adaptation.

785 Nat. Rev. Genet. **14**: 807–820. doi:10.1038/nrg3522

786 Schoepf, V., M. Stat, J. L. Falter, and M. T. McCulloch. 2015. Limits to the thermal tolerance  
787 of corals adapted to a highly fluctuating, naturally extreme temperature environment.  
788 Sci. Rep. **5**: 17639. doi:10.1038/srep17639

789 Smale, D. A., and others. 2019. Marine heatwaves threaten global biodiversity and the  
790 provision of ecosystem services. Nat. Clim. Chang. **9**: 306–312. doi:10.1038/s41558-  
791 019-0412-1

792 Smith, S. V., and G. S. Key. 1975. Carbon dioxide and metabolism in marine environments.  
793 Limnol. Oceanogr. **20**: 493–495.

794 Soetaert, K., T. Petzoldt, F. Meysman, and L. Meire. 2020. marelac : Tools for aquatic  
795 sciences. R package version 2.1.10. <https://cran.r-project.org/package=marelac>.

796 Teixidó, N., M. C. Gambi, V. Parravacini, K. Kroeker, F. Micheli, S. Villéger, and E.  
797 Ballesteros. 2018. Functional biodiversity loss along natural CO<sub>2</sub> gradients. Nat.  
798 Commun. **9**: 1–9. doi:10.1038/s41467-018-07592-1

799 Teixidó, N., and others. 2020. Ocean acidification causes variable trait-shifts in a coral  
800 species. Glob. Chang. Biol. **26**: 6813–6830. doi:10.1111/gcb.15372

801 Trotter, J., and others. 2011. Quantifying the pH “vital effect” in the temperate zooxanthellate  
802 coral *Cladocora caespitosa*: Validation of the boron seawater pH proxy. Earth Planet.  
803 Sci. Lett. **303**: 163–173. doi:10.1016/j.epsl.2011.01.030

804 Varnerin, B., B. Hopkinson, and D. Gleason. 2020. Recruits of the temperate coral *Oculina*  
805 *arbuscula* mimic adults in their resilience to ocean acidification. Mar. Ecol. Prog. Ser.  
806 **636**: 63–75. doi:10.3354/meps13228

807 Wall, M., and others. 2019. Linking internal carbonate chemistry regulation and calcification

808 in corals growing at a Mediterranean CO<sub>2</sub> vent. *Front. Mar. Sci.* **6**: 1–12.

809 doi:10.3389/fmars.2019.00699

810 Wang, C., E. M. Arneson, D. F. Gleason, and B. M. Hopkinson. 2020. Resilience of the  
811 temperate coral *Oculina arbuscula* to ocean acidification extends to the physiological  
812 level. *Coral Reefs*. doi:10.1007/s00338-020-02029-y

813 Zibrowius, H. 1995. The “Southern” *Astroides calycularis* in the Pleistocene of the northern  
814 Mediterranean—An indicator of climatic changes (Cnidaria, scleractinia). *Geobios* **28**:  
815 9–16. doi:10.1016/S0016-6995(95)80201-0

816

## 817 **Acknowledgements**

818 This research was supported by the French Government through the National Research  
819 Agency - Investments for the Future (“4Oceans-Make Our Planet Great Again” grant, ANR-  
820 17-MPGA-0001). Thanks are due to the *Service d’Observation Rade de Villefranche* (SO-  
821 Rade) of the *Institut de la mer de Villefranche* and the *Service d’Observation en Milieu*  
822 *Littoral* (SOMLIT/CNRS-INSU) for their kind permission to use the Point B data. We thank  
823 Samir Alliouane for assistance in the laboratory and P. Sorvino (ANS Diving, Ischia) for  
824 assistance in the field.

## 825 **Author contributions**

826 S.C., N.T., B.M., and J.-P.G designed the study. N.T., S.C., A.M. and B.M. were involved with  
827 fieldwork. C.C, B.M., T.G., S.C., and N.T performed the experiments. C.C., N.T. and A.M.  
828 analyzed the data. C.C. wrote the first draft of the manuscript which was then finalized by all  
829 co-authors.